Biophysical Properties, Pharmacology, and Modulation of Human, Neuronal L-Type (α_{1D}, $Ca_V1.3$) Voltage-Dependent Calcium Currents

D. C. BELL,[1] A. J. BUTCHER,[1] N. S. BERROW,[1] K. M. PAGE,[1] P. F. BRUST,[2] A. NESTEROVA,[2] K. A. STAUDERMAN,[2] G. R. SEABROOK,[3] B. NÜRNBERG,[4] AND A. C. DOLPHIN[1]
[1]*Department of Pharmacology, University College London, London WC1E 6BT, United Kingdom;* [2]*Merck Research Laboratories, La Jolla, California 92307;* [3]*Abteilung Pharmakologie und Toxikologie, Universität Ulm and Institut für Pharmakologie, Freie Universität, D-14195 Berlin, Germany; and* [4]*Merck, Sharp and Dohme, Neuroscience Research Centre, Harlow CM20 2QR, United Kingdom*

Received 17 May 2000; accepted in final form 18 October 2000

Bell, D. C., A. J. Butcher, N. S. Berrow, K. M. Page, P. F. Brust, A. Nesterova, K. A. Stauderman, G. R. Seabrook, B. Nürnberg, and A. C. Dolphin. Biophysical properties, pharmacology, and modulation of human, neuronal L-type (α_{1D}, $Ca_V1.3$) voltage-dependent calcium currents. *J Neurophysiol* 85: 816–827, 2001. Voltage-dependent calcium channels (VDCCs) are multimeric complexes composed of a pore-forming α_1 subunit together with several accessory subunits, including $\alpha_2\delta$, β, and, in some cases, γ subunits. A family of VDCCs known as the L-type channels are formed specifically from α_{1S} (skeletal muscle), α_{1C} (in heart and brain), α_{1D} (mainly in brain, heart, and endocrine tissue), and α_{1F} (retina). Neuroendocrine L-type currents have a significant role in the control of neurosecretion and can be inhibited by GTP-binding (G-) proteins. However, the subunit composition of the VDCCs underlying these G-protein–regulated neuroendocrine L-type currents is unknown. To investigate the biophysical and pharmacological properties and role of G-protein modulation of α_{1D} calcium channels, we have examined calcium channel currents formed by the human neuronal L-type α_{1D} subunit, coexpressed with $\alpha_2\delta$-1 and β_{3a}, stably expressed in a human embryonic kidney (HEK) 293 cell line, using whole cell and perforated patch-clamp techniques. The α_{1D}-expressing cell line exhibited L-type currents with typical characteristics. The currents were high-voltage activated (peak at +20 mV in 20 mM Ba^{2+}) and showed little inactivation in external Ba^{2+}, while displaying rapid inactivation kinetics in external Ca^{2+}. The L-type currents were inhibited by the 1,4 dihydropyridine (DHP) antagonists nifedipine and nicardipine and were enhanced by the DHP agonist BayK S-(−)8644. However, α_{1D} L-type currents were not modulated by activation of a number of G-protein pathways. Activation of endogenous somatostatin receptor subtype 2 (sst2) by somatostatin-14 or activation of transiently transfected rat D2 dopamine receptors ($rD2_{long}$) by quinpirole had no effect. Direct activation of G-proteins by the nonhydrolyzable GTP analogue, guanosine 5′-0-(3-thiotriphospate) also had no effect on the α_{1D} currents. In contrast, in the same system, N-type currents, formed from transiently transfected $\alpha_{1B}/\alpha_2\delta$-$1/\beta_3$, showed strong G-protein–mediated inhibition. Furthermore, the I–II loop from the α_{1D} clone, expressed as a glutathione-S-transferase (GST) fusion protein, did not bind $G\beta\gamma$, unlike the α_{1B} I–II loop fusion protein. These data show that the biophysical and pharmacological properties of recombinant human α_{1D} L-type currents are similar to α_{1C} currents, and these currents are also resistant to modulation by $G_{i/o}$-linked G-protein–coupled receptors.

INTRODUCTION

The L-type voltage-dependent calcium channels (VDCCs) are formed by one of four possible pore forming α_1 subunits: α_{1S} (found in skeletal muscle) (Tanabe et al. 1987), α_{1C} (mainly cardiac) (Mikami et al. 1989), α_{1D} (in neurons and neurosecretory cells and heart) (Seino et al. 1992; Williams et al. 1992; Wyatt et al. 1997; Yaney et al. 1992), or α_{1F} (retinal, not yet functionally expressed) (Strom et al. 1998). The VDCC family nomenclature was recently revised by Ertel et al. (2000): α_{1S}, α_{1C}, α_{1D}, and α_{1F} were renamed $Ca_V1.1$, $Ca_V1.2$, $Ca_V1.3$, and $Ca_V1.4$, respectively. The α_1 subunits are coassembled with the accessory subunits β, $\alpha_2\delta$ (and γ_1 in skeletal muscle). L-type currents have been defined pharmacologically by their sensitivity to low (nM to μM) concentrations of 1,4-dihydropyridine (DHP) antagonists (e.g., nifedipine and nicardipine) and agonists [e.g., S-(−)BayK8644] (Sanguinetti and Kass 1984). In addition, L-type channels exhibit the following biophysical characteristics: "long-lasting" currents that show little inactivation in Ba^{2+} (Nowycky et al. 1985); some selectivity for Ba^{2+} over Ca^{2+} and Ca^{2+}-dependent inactivation (Soldatov et al. 1997).

GTP-binding (G-) proteins exist as heterotrimeric complexes, composed of a $G\alpha$ subunit and a $G\beta\gamma$ dimer. On activation of a G-protein–coupled receptor (GPCR), the heterotrimer dissociates into free $G\alpha$-GTP and $G\beta\gamma$ dimers. It is these free $G\beta\gamma$ subunits that are thought to be responsible for fast, membrane delimited, voltage-dependent G-protein inhibition of certain neuronal VDCCs, including α_{1A}, α_{1B}, and α_{1E} (Herlitze et al. 1996; Ikeda 1996; Page et al. 1998; for a review see Dolphin 1998). VDCCs undergoing voltage-dependent G-protein modulation display the following characteristics: a decrease in whole cell current, depolarizing shift in the current-voltage (*I-V*) relationship, and slowed activation kinetics (Bean 1989). Another characteristic is the loss of G-protein modula-

Address for reprint requests: A. C. Dolphin, Dept. of Pharmacology (Medawar Building), University College London, Gower St., London WC1E 6BT, UK (E-mail: a.dolphin@ucl.ac.uk).

The costs of publication of this article were defrayed in part by the payment of page charges. The article must therefore be hereby marked "*advertisement*" in accordance with 18 U.S.C. Section 1734 solely to indicate this fact.

tion at large depolarizations (Bean 1989); consequently a large depolarizing prepulse immediately before a test pulse transiently removes inhibition, and the activation kinetics become faster, a phenomenon termed prepulse facilitation (Bean 1989; Elmslie et al. 1990).

Native cardiac L-type channels have long been known to exhibit G-protein-induced stimulation via $G\alpha_S$ and a cAMP-dependent protein kinase pathway (Reuter 1983). Recently stimulation of smooth muscle L-type currents by $G\beta\gamma$ has also been reported via a phosphinositide 3 kinase pathway (Viard et al. 1999). Inhibition via activation of $G\alpha_{i/o}$, and subsequent inhibition of adenylyl cyclase, is another G-protein modulatory path that regulates cardiac L-type channels (Fischmeister and Hartzell 1986). In native endocrine and neurosecretory cells and cell lines, G-protein inhibition of L-type currents has also been observed (Degtiar et al. 1997; Gilon et al. 1997; Haws et al. 1993; Hernandez-Guijo et al. 1999; Kleuss et al. 1991; Mathie et al. 1992; Tallent et al. 1996). This is thought to be involved in the inhibitory modulation of secretion. However, the subtype(s) of VDCC α_1 subunit(s) involved and type of G-protein modulation observed for these L-type currents have not been fully defined (see Dolphin 1999, for review). In neuronal and neurosecretory tissue, L-type currents are formed from α_{1D} as well as α_{1C} subunits (Chin et al. 1992). α_{1D} has also been shown to be expressed in heart (Hell et al. 1993; Wyatt et al. 1997). The consensus of current research suggests that L-type currents resulting from expression of neuronal (Bourinet et al. 1996; Canti et al. 1999) or cardiac (Meza and Adams 1998) α_{1C} isoforms do not exhibit the voltage-dependent G-protein inhibition that is typical of N or P/Q currents. Nevertheless, in experiments where cloned α_{1C} has been co-expressed with accessory subunits in *Xenopus laevis* oocytes (Oz et al. 1998) and HEK 293 cells (Dai et al. 1999; Kamp et al. 2000), other forms of facilitation and second-messenger–based inhibition have been observed.

The existence of G-protein modulation of cloned α_{1D} L-type VDCCs has not yet been examined. Here we have used a stable HEK 293 cell line expressing the human α_{1D} subunit, together with the human accessory subunits $\alpha_2\delta$-1 and β_{3a}, to establish the biophysical and pharmacological properties of the expressed current and whether the resultant current shows G-protein modulation.

METHODS

Materials

The following compounds were stored at −20°C (stock concentration in mM unless stated, solvent, and source): nifedipine, NIF (3, ethanol, Sigma, St. Louis, MO); nicardipine, NIC (3, ethanol, Sigma); BayK S-(−)8644, BayK (3, ethanol, RBI, Natwick, MA); somatostatin-14, SST (0.1, deoxygenated double-distilled water, RBI, Natwick, MA); quinpirole, Quin (10, double-distilled water, RBI); forskolin (10, dimethyl sulfoxide, Sigma); geneticin G-418 sulfate (100 mg/ml, double-distilled water, Life Technologies, Paisley, Scotland); Zeocin (100 mg/ml, supplied in solution form, Invitrogen, Carlsbad, CA); and amphotericin-B (80 mg/ml, dimethyl sulfoxide, Sigma).

The following cDNAs were used in transient transfections: rabbit α_{1B} (GenBank accession number D14157), rat α_{1E} (rbEII, L15453), rat $\alpha_{1E\ long}$ (see below for details), rat β_{1b} (Tomlinson et al. 1993), rat β_3 (M88571), rat $\alpha_2\delta$-1 (neuronal splice variant, M86621), rat $D2_{long}$ receptor ($rD2_{long}$, X17458, N5 → G), and mut-3 green fluorescent protein (GFP, U73901). All cDNAs were subcloned into the expression vector pRK5 except for the clones used in the $\alpha_{1E\ long}$ transient transfection study, which were subcloned into the expression vector pMT2 (Genetic Institute, Cambridge, MA) (see Swick et al. 1992). The rat α_{1E} (rbEII, L15453) clone has a truncated N-terminus, compared with other α_{1E} clones. Page et al. (1998) extended this clone using a rat α_{1E} N-terminal extension (AF057029). The resulting rat $\alpha_{1E\ long}$ clone used in this study has homology to published mouse (L29346), human (L27745), and rabbit (X67855) α_{1E} clones. The β_{1b} subunit used in this study is that of Tomlinson et al. (1993). It is identical to the rat β_{1b} clone defined in the GenBank database (X61394) except for two substitutions (R417 → S and V435 → A) and the deletion A431 (T. P. Snutch, personal communication).

α_{1D} Stable cell line (HEK 293 α1D)

Standard techniques were used to transfect HEK 293 stably with human neuronal α_{1D} (M76558), $\alpha_{2b}\delta$-1 (M76559) and β_{3a} (not published); for clarity this cell line (#5D12-20) will subsequently be referred to as HEK 293 α_{1D}. The cloning of these VDCC subunits is discussed in Williams et al. (1992). The clonal α_{1D} cell line was established by transfecting HEK293 cells using a standard Ca^{2+} phosphate procedure (Brust et al. 1993) with 10, 5, and 5 μg of the α_{1D}, $\alpha_{2b}\delta$-1, and β_{3a} expression constructs, respectively. The α_{1D} subunit expression plasmid, pcDNA1α_{1D}RBS, does not contain an antibiotic resistance gene, whereas the $\alpha_{2b}\delta$-1 and β_{3a} subunit expression plasmids, pRc/CMV$\alpha_{2b}\delta$-1 and pZeoCMVβ_{3a}, contain the neomycin and Zeocin resistance genes, respectively. Geneticin G-418 sulfate (final concentration 100 μg/ml, Life Technologies) and Zeocin (final concentration 40 μg/ml, Invitrogen) were used for selection of colonies. The selection medium was added to the cells 48 h after transfection. Antibiotic-resistant colonies were transferred to 96-well plates using cloning cylinders, 2–4 wk after selection was initiated. Cell lines containing functional channels were selected with a fluo3-based calcium flux assay.

Cell culture and transfection

The culture medium in which the HEK 293 α_{1D} and control HEK 293 cells were grown consisted of Dulbecco's modified Eagle's medium (DMEM) with 4.5-g glucose $\cdot$ l^{-1} (DMEM, Life Technologies). This was supplemented with 5% bovine calf serum (Hyclone, UT), penicillin (100 IU $\cdot$ ml^{-1}) and streptomycin (100 $\mu g \cdot ml^{-1}$; Life Technologies) and the additional selection antibiotics for the HEK 293 α_{1D} cell line (as described above). The cells were grown in this medium at 37°C, 5% CO_2, and passaged every 2–3 days.

For transient transfection of the α_{1B}, $\alpha_2\delta$-1, β_{3a} VDCC subunits and mut-3 GFP expression marker into HEK 293 cells, a mixture was made containing, respectively, 15, 5, 5, and 1 μl of the cDNAs (at a concentration of 1 $\mu g/\mu l$). In experiments where the $rD2_{long}$ was used, 5 μg of this cDNA was added; in experiments where this D2 receptor pathway was not investigated, 5 μg of blank pRK5 vector was used to give a final cDNA amount of 31 μg. The same amounts were used for the transfection of α_{1E}, $\alpha_2\delta$-1, β_{1b}, and mut-3 GFP (using 5 μg of blank pMT2 to make the mixture up to a final amount of 31 μg). For transfection, 10 μl of Geneporter reagent (Genetic Therapy Systems, San Diego, CA) and 2 μl of the cDNA mix were added to each 1 ml of DMEM (no supplements) and incubated at 20°C for 1 h before addition of 1 ml to each 35-mm-diam culture dish containing approximately 2×10^6 cells. Transfected cells were then grown at 37°C for 36 h and subsequently at 28°C for 36 h. This process of 37°C/28°C incubation was also the standard procedure for the stable α_{1D} cell line before electrophysiological experiments. In experiments on the HEK 293 α_{1D} cells where additional transient transfection of $rD2_{long}$ expression was required, the cDNA mix was formed of $rD2_{long}$ (5 μg) and mut-3 GFP (1 μg) cDNA, and made up to 31 μg with blank pRK5, with the transfection procedure being as described above (for

α_{1B} and α_{1E}). Successful transfection was determined by expression of mut3-GFP.

Electrophysiology

The internal (pipette) and external solutions and recording techniques were similar to those previously described (Campbell et al. 1995). For whole cell patch-clamp recordings, the patch pipette solution contained (in mM) 140 Cs-aspartate, 5 EGTA, 2 $MgCl_2$, 0.1 $CaCl_2$, 2 K_2ATP, 0.8 TrisGTP, 10 HEPES; pH 7.2, 310 mOsm with sucrose. In experiments where guanosine 5′-0-(3-thiotriphospate) (GTP-γS) and guanosine 5′-0-(2-thiodiphospate) (GDP-βS) were used, the GTP was replaced with either 100 μM GTP-γS (Sigma) or 2 mM GDP-βS (Boehringer, Mannheim, Germany). For perforated-patch clamp recordings the patch pipette solution contained (in mM) 100 CH_3O_3SCs, 25 CsCl, 3 $MgCl_2$, 40 HEPES; pH 7. 3, and freshly supplemented (within 1 h of recording) with 240 μg/ml amphotericin-B. The external solution contained (in mM) 160 tetraethylammonium (TEA) bromide, 3 KCl, 1.0 $NaHCO_3$, 1.0 $MgCl_2$, 10 HEPES, 4 glucose, 10 or 20 $BaCl_2$ or $CaCl_2$; pH 7. 4, 320 mOsm with sucrose. The perfusion rate was 1–2 ml/min. Pipettes of resistance 2–5 MΩ were used. An Axon 200A or an Axopatch 1D amplifier (Axon Instruments, Foster City, CA) was used, and data were filtered at 1 kHz and digitized at 5–10 kHz using a Digidata 1200 interface (Axon Instruments). Membrane capacitance measurements were recorded from the amplifier following capacitance compensation. Analysis was performed using pClamp 6.02 (Axon Instruments) and Origin 5 (Microcal Software, Northampton, MA). Current records are shown following leak and residual capacitance current subtraction (P/4 or P/5 protocol). Data are expressed as means ± SE. Statistical analysis was performed using paired or unpaired Student's *t*-test, as appropriate, where significance was defined as $P < 0.05$ (*) and $P < 0.01$ (**). Where indicated, *I-V* relations were fitted with a combined Boltzmann and linear fit

$$I_V = G_{max}(V - V_{rev})/\{1 + \exp[-(V - V_{50,act})/k]\} \quad (1)$$

where I_V is the current density at voltage V, G_{max} is the maximum conductance · pF^{-1}, $V_{50,act}$ is the mid-point of voltage dependence of activation, V_{rev} is the reversal potential, and k is the slope factor.

Steady-state inactivation data were fitted with a Boltzmann function of the form

$$I_V/I_{max} = 1/\{1 + \exp[(V - V_{50,inact})/k]\} \quad (2)$$

where I_V/I_{max} is the current normalized to maximum current, $V_{50,inact}$ is the mid-point of voltage dependence of inactivation, V is the conditioning potential, and k is the slope factor. Current activation was fitted with a similar Boltzmann function with I_V/I_{max} substituted by G_V/G_{max} (normalized conductance) and $V_{50,inact}$ substituted by $V_{50,act}$.

The holding potential was −80 mV, unless otherwise stated. Voltages were not corrected for liquid junction potential, measured using the method described in Neher (1995), which were up to −2.7 mV in whole cell recording solutions and −5.4 mV in perforated-patch solutions.

Construction, expression, and purification of proteins

The polymerase chain reaction (PCR) was used to amplify (from full length clones) regions of cDNA encoding the calcium channel I–II loops of the rabbit α_{1B} and human α_{1D} clones (M76558). As the full length clone of the human α_{1D} was unavailable for PCR, it was necessary to perform RT-PCR from the HEK 293 α_{1D} cell line. Approximately 10^5 HEK 293 α_{1D} cells were lysed using the QiaShredder and the total RNA extracted using the Qiagen RNEasy kit (Qiagen, Crawley, UK). After a further phenol/chloroform extraction and precipitation the total RNA was reverse transcribed using MMLV-Reverse Transcriptase (Life Technologies, Paisley, Scotland) and random hexamer primers (Promega, Southampton, UK). PCR was performed using either *Pfu* (Promega) or *Pfx* (Life Technologies) high-fidelity DNA polymerase in the supplied polymerase buffers. *Bam*HI and *Eco*RI restriction sites (underlined) for directional, in-frame cloning of the resulting fragments into pGEX2T (Pharmacia, St. Albans, UK) were present in the primer sets as follows:

α_{1B} Forward: 5′CTCA*GGATCC*TTTGCTAAGGAGCG3′
Reverse: 5′AGAA*GAATTC*TGCCTTCACCATGC3′
α_{1D} Forward: 5′GT*GGATCC*TTCTCAAAGGAAAGAG3′
Reverse: 5′AG*GAATTC*GTGACAGACTTCAC3′

Amplification was for 30 cycles before the resulting products were separated by agarose gel electrophoresis, digested with *Bam*HI and *Eco*RI and subcloned into pGEX2T (Pharmacia). The resulting constructs are GSTα_{1B}I–II loop and GSTα_{1D}I–II loop, respectively. The sequences of all the fusion protein constructs were verified by cycle sequencing (Sequitherm, Epicentre laboratories, Madison, WI) or automated sequencing, before use in protein expression studies.

Expression cultures of BL21(DE3)-Codon Plus-(RIL) *Escherichia coli* (Stratagene, Amsterdam, NL) were grown overnight at 37°C in LB medium supplemented with 34 μg/ml chloramphenicol, 50 μg/ml ampicillin, and 1% (wt/vol) glucose. The saturated cultures were diluted 10-fold in the same medium and grown for a further 2.5 h. before cooling to 25°C and induction with 0.1 mM isopropyl-thio-galactopyranoside. Induced cultures were grown at 25°C for a further 2.5 h before harvesting. All further purification steps were performed at 4°C. Cells were lysed by sonication in phosphate-buffered saline, pH 7.4 (PBS: 10 mM phosphate buffer, pH 7.4, 137 mM NaCl, 2.7 mM KCl) containing 1% sarcosyl, 25 mM EDTA, 0.5 mM dithiothreitol, and protease inhibitors (1 tablet per 50 ml of lysate, Complete EDTA-free, Roche Diagnostics, Lewes, UK) followed by a 10-min incubation at 4°C. TritonX-100 was then added to a final concentration of 2% and the lysate re-sonicated and incubated at 4°C for a further 10 min. before centrifugation at 20,000 × *g* for 15 min at 4°C. The resulting supernatant was then applied to a 1-ml GSTrap column (Pharmacia) and the column washed with 10 column volumes of binding buffer (PBS, pH 7.4 containing 0.1% Triton X100, 20 mM EDTA, 0.5 mM dithiothreitol and 1 protease inhibitor tablet per 200 ml). Bound GST-fusion proteins were then eluted from the column with elution buffer (binding buffer, at pH 8.0, supplemented with 5 mM reduced glutathione). Glutathione was removed from the fusion protein preparations by dialysis against HBS-EP buffer [10 mM HEPES, pH 7.4, 150 mM NaCl, 3 mM EDTA, 0.005% (vol/vol) Tween 20] before samples were frozen in aliquots at −20°C.

Bovine brain G-proteins were purified to apparent homogeneity using conventional chromatographic techniques. G$\beta\gamma$ dimers were then liberated from Gα subunits in the presence of aluminum fluoride (Exner et al. 1999). Isolation and final purification of G$\beta\gamma$ was achieved using a Mono Q FPLC column (Pharmacia). G$\beta\gamma$ subunits were identified by their immunoreactivity and stored in aliquots at −80°C until required for use.

A full-length β_{1b} with C-terminal hexa-histidine tag (H6Cβ_{1b}) was produced by PCR (10 cycles) using *Pfu* polymerase (Stratagene, Amsterdam), β_{1b} in pMT2 as template and the following primers:

Forward: 5′GGGAATTCATGGTCCAGAAGAGCG3′
Reverse: 5′ GGGAATTCTCAATGATGATGATGATGATGGCGGATCTACACG 3′

The resulting PCR product (approximately 1.9k.b.) was digested with *Eco*RI and subcloned into the pKK233–3 vector (Amersham Pharmacia, Little Chalfont, UK). To maximize yields of the full-length H6Cβ_{1b} protein the 600b.p. 3′ *Nco*I-*Eco*RI fragment of H6Cβ_{1b} and the 1.3k.b. 5′*Nco*I-*Nco*I fragment of β_{1b} were subcloned into *Nco*I-*Eco*RI digested pET28b (Novagen, Nottingham, UK) to give H6Cβ_{1b}-pET28b. BL21(DE3)-Codon Plus-(IRL) *Escherichia coli* (Stratagene) were transformed with H6Cβ_{1b}-pET28b, and cultures were grown overnight to saturation at 37°C in LB (pH 5.5) supplemented with kanamycin (30 μg/ml), chloramphenicol (34 μg/

ml) and 1% wt/vol glucose, diluted 1:10 with the same media and grown for a further 3 h before cooling to room temperature and induction with 0.5 mM isopropylthio-β-D-galactoside (IPTG). The cultures were grown for 3 h postinduction at room temperature then harvested by centrifugation, pellets were stored at −70°C until required.

Escherichia coli pellets containing expressed H6Cβ_{1b} protein were lysed at 4°C by sonication in 20 mM phosphate buffer (pH 7.4), containing 1 protease inhibitor tablet per liter of culture pelleted. Solid NaCl was added to the lysate to a final concentration of 1 M before the lysate was cleared at 20,000 × *g* at 4°C for 15 min. Imidazole solution (pH 7.4) was then added to the resulting supernatant to give a final concentration of 40 mM before loading onto a nickel-primed 5 ml HiTrap Chelating column (Amersham Pharmacia) equilibrated with loading buffer (20 mM phosphate buffer, pH 7.4, 1 M NaCl, 40 mM Imidazole, 0.15% wt/vol octylglucoside and 1 protease inhibitor tablet per 100 ml). The column was washed thoroughly with wash buffer (as load buffer but 70 mM imidazole) before H6Cβ_{1b} was eluted from the column in elution buffer (as load buffer but 200 mM imidazole).

Peak UV_{280} absorbance fractions were rapidly buffer exchanged on a Sephadex G-25 (Amersham Pharmacia) column into IEX buffer (20 mM 2-[N-morpholino]ethanesulfonic acid, pH 6.0, 1 protease inhibitor tablet per 200 ml) supplemented with 500 mM NaCl, before dilution 1:10 with IEX buffer. The diluted sample was loaded onto a 1 ml SP-Sepahrose HP column (Amersham Pharmacia), the column was washed with IEX buffer before H6Cβ_{1b} proteins were eluted in a linear gradient of 0 to 1 M NaCl in IEX buffer. Fractions containing H6Cβ_{1b} were identified by SDS-PAGE analysis, with Coomassie blue staining, before dialysis against storage buffer (20 mM borate, pH 8.0, 500 mM NaCl, 1 mM EDTA, 1 protease inhibitor tablet per 200 ml). H6Cβ_{1b} prepared in this manner was found to have a half-life in excess of 60 days at 4°C as judged by SDS-PAGE and Coomassie blue staining.

Surface plasmon resonance binding assay

All assays were performed on a Biacore 2000 (Biacore AB, Uppsala, Sweden) at 25°C in HBS-EP buffer (10 mM HEPES, pH 7.4; 150 mM NaCl, 3 mM EDTA, 0.005% vol/vol polysorbate 20) unless stated otherwise. Glutathione S-transferase (GST) fusion proteins were immobilized on CM5 dextran chips using an anti-GST monoclonal antibody kit according to the manufacturer's instructions (Biacore AB). To obtain identical molar loadings of the different molecular mass fusion proteins, the following resonance unit (RU) correction factors were used during immobilization (GST = 1, GSTα_{1D}I–II loop = 1.52, GSTα_{1B}I–II loop = 1.57). G$\beta\gamma$ dimers were diluted in HBS-EP buffer before use, and G$\beta\gamma$ injections were performed using a flow rate of 50 μl/min for 5 min. Experiments using H6Cβ_{1b} were performed in modified HBS-EP buffer containing 500 mM NaCl, with the same flow rate and injection time used for the G$\beta\gamma$ experiments.

RESULTS

α_{1D} Sensitivity to DHPs

From electrophysiological recording of the HEK 293 α_{1D} ($\alpha_{1D}/\alpha_2\delta$-1/$\beta_{3a}$) cell line, 43% of cells were found to express calcium channel currents, and for those currents that were stable, the mean current density was −10 ± 2.1 pA/pF (mean ± SE, n = 21) in 20 mM Ba^{2+} at a test potential of +10 mV (and approximately half this value when recorded in 10 mM Ba^{2+}). As expected, the α_{1D} currents displayed sensitivity to DHP antagonists. The effects of 3 and 10 μM nifedipine are shown in the time course in Fig. 1*A*, and the percentage inhibition of I_{Ba} by 3 μM nifedipine and nicardipine is shown in the bar chart in Fig. 1*B*. The 1,4-DHP antagonist block was also characterized by an increase in the inactivation kinetics of I_{Ba} during the test depolarization (+10 mV, V_t), which can be observed by comparing the inhibition at peak compared with the end of the 200-ms test pulse (○ and ●, respectively, in Fig. 1*A*, and □ and ■ in Fig. 1*B*). However, α_{1D} I_{Ba} showed very similar inhibition by nifedipine at three different holding potentials (V_h = −80, −50, and −30 mV). At V_h = −50 mV, 3 μM nifedipine inhibited α_{1D} I_{Ba} by 62 ± 7% (at peak) and 94 ± 3% (at the end of 200 ms pulse, n = 5); at V_h = −30 mV the inhibition was similar, being 56 ± 7% (at peak) and 91 ± 3% (at 200 ms, n = 6).

The agonist BayK S-(−)8644 (3 μM) produced a marked enhancement of the current (325 ± 25% increase, n = 5, at V_t = +10 mV in 10 mM Ba^{2+}; 680 ± 84% increase, n = 14, at V_t = +10 mV in 20 mM Ba^{2+}; Fig. 1*C*). The onset of enhancement was rapid (reaching steady-state enhancement within 1–2 min of application, Fig. 1*C*) and was accompanied by a characteristic hyperpolarizing shift in the *I-V* relationship (Fig. 1*D*). In some recordings BayK S-(−)8644 enhanced α_{1D} currents also displayed the characteristic slowing of tail current deactivation (for an example, see the enhanced current trace in Fig. 6*B*).

Biophysical characteristics of the α_{1D} current

The activation and steady-state inactivation of α_{1D} currents are shown in Fig. 2*A*. Fitting the current activation gave a $V_{50,act}$ of +1.8 ± 1.2 mV. Examining the steady-state inactivation properties of the α_{1D} currents showed that at test potentials up to +30 mV the α_{1D} currents did not fully inactivate and had a relatively depolarized $V_{50,inact}$ of −13. 4 ± 1.8 mV (n = 6). The inactivation kinetics at V_t = +10 mV were very slow in Ba^{2+} (see examples of control traces in Fig. 1, *A*, *C*, and *D*). Single exponentials were fitted to the inactivating phase during long (1,200–1,600 ms) depolarizing steps, (e.g., the white line in the example trace shown in Fig. 2*B*). The τ_{inact} was 439 ± 50 ms (n = 4). The inactivation kinetics with external Ca^{2+} rather than Ba^{2+} were far more rapid, shown by the overlaid example traces in Fig. 2*C*. Almost complete inactivation was observed during a 200-ms depolarizing pulse in Ca^{2+} (τ_{inact} = 44.3 ± 1.1 ms, n = 7). Additionally, the peak current in 20 mM Ca^{2+} was smaller than in 20 mM Ba^{2+} (I_{Ca} was ~20% of I_{Ba}). The mean *I-V* relationship in 20 mM Ba^{2+} and 20 mM Ca^{2+} exemplifies these differences (Fig. 2*D*).

α_{1D} Currents do not show G-protein–mediated inhibition

Having established some basic biophysical and pharmacological properties of α_{1D} currents, we then examined whether these currents displayed G-protein modulation. Initially the modulation of the α_{1D} currents was compared with that of α_{1B} currents (known to be G-protein modulated), transiently expressed in HEK 293 cells, by activating the endogenous somatostatin receptor subtype 2 (sst2). Application of somatostatin (SST, 100–500 nM, n = 8) had no effect on the α_{1D} current (Fig. 3*A*). Using the same endogenous receptor-based signaling pathway, application of SST (500 nM) caused a rapid inhibition of α_{1B} currents, observed in all cells tested (see Fig. 3*B;* mean inhibition, 40 ± 7%, n = 8).

Due to the nature of whole cell patch clamping, the internal

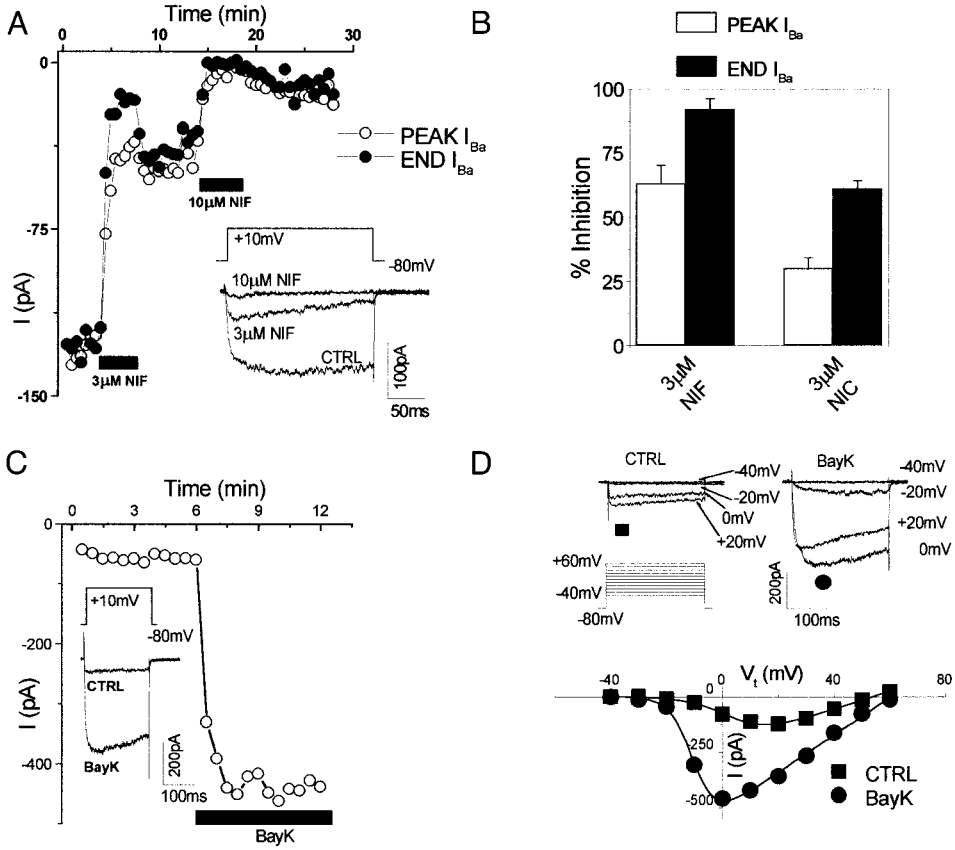

FIG. 1. The α_{1D} currents are sensitive to 1,4 dihydropyridines (DHPs). *A*: the α_{1D} currents show inhibition by the DHP antagonist nifedipine (NIF). Time course of currents measured at peak (○) and at the end (●) of the 200-ms test pulse. Depolarizing test pulses ($V_t = +10$ mV) were given every 30 s from a holding potential (V_h) of −80 mV. Application of NIF (3 and 10 μM) are denoted by the horizontal bars. The *inset* shows example traces taken from the time course for control (CTRL, 10 mM Ba^{2+}) and for 3 and 10 μM NIF; the test pulse protocol is above these example traces. *B*: bar graph depicting mean current inhibition (%) at peak (□) and end of the 200 ms test pulse (■) for nifedipine (NIF, 3 μM, $n = 7$) and nicardipine (NIC, 3 μM, $n = 6$). *C*: sensitivity of α_{1D} currents to the DHP agonist S(−)-BayK8644. An example time course of measured peak current (○) recorded with step depolarizations from $V_h = -80$ mV to $V_t = +10$ mV, at 30-s intervals (see pulse protocol above *inset* of example traces). Application of S(−)-BayK8644 (3 μM) is denoted by the horizontal bar below time course. *D*: an example cell showing a family of current-voltage (*I-V*) traces in control (20 mM Ba^{2+}; CTRL) and during S(−)-BayK8644 (3 μM; BayK) enhancement of the current. *I-V* families were formed by depolarizing from −80 mV to between −40 and +60 mV in 10-mV increments, every 5 s (see pulse protocol below the CTRL family of traces). For clarity example traces are shown for currents measured by stepping to −40, −20, 0, and +20 mV only. In each condition, peak current was measured and plotted as an *I-V* relationship (*bottom;* CTRL, ■; with BayK, ●) and fitted by a modified Boltzmann equation (*Eq. 1*, see METHODS).

contents of the cell can be disrupted, resulting in loss of normal signaling pathways within the cell. Such "wash out" effects can be minimized by using the perforated-patch clamp technique (Horn and Marty 1988). To ensure that the loss of G-protein modulation was not due to such wash out, amphotericin-B perforated patches were also used; however, no modulation of α_{1D} currents by SST was observed at any test potential ($n = 5$, Fig. 3*C*). *I-V* relationship pulse protocols were performed during control, SST perfusion and wash conditions in a perforated patch-clamp recording (example traces from these *I-V* relationships are shown at the *bottom* of Fig. 3*C*). The results exemplify the lack of effect of SST with almost identical values for $V_{50,act}$ (CTRL = −6.1 mV; SST = −6.6 mV; WASH = −5.7 mV) and k (CTRL = 8.6 mV; SST = 8.2 mV; WASH = 8.4 mV).

To examine another G-protein–coupled receptor pathway, the $rD2_{long}$ receptor was transiently co-expressed with GFP as an expression marker in the α_{1D} cell line and was also transiently co-expressed with $\alpha_{1B}/\alpha_2\delta\text{-}1/\beta_3$ in HEK293 cells. However, application of the D2 agonist quinpirole (300 nM), had no effect on α_{1D} currents ($n = 7$, Fig. 4*A*), although a clear inhibitory effect was observed in 10/16 of the $\alpha_{1B}/\alpha_2\delta\text{-}1/\beta_3$ expressing cells (with a mean inhibition of 59 ± 7%, $n = 10$; Fig. 4*B*). This inhibition was greater than that produced by activation of the endogenous sst2 receptor, suggesting more efficient activation of this G-protein pathway by D2 receptors, but despite this, no inhibition of α_{1D} currents was observed (Fig. 4*C*).

The GTP analogue GTP-γS can be used as a more direct way of activating G-proteins since it is nonhydrolyzable and leads to their sustained activation. Conversely, the GDP analogue GDP-βS can be used to block G-protein activation. Using these guanine nucleotide analogues, the existence of tonic modulation was examined with a prepulse (PP) protocol. Figure 5*A* depicts the ratio of current in the absence (no PP) or immediately following (+PP) a large depolarizing prepulse (+PP/no PP ratio) for control (CTRL, gray columns and associated example traces), with 100 μM GTP-γS (black columns

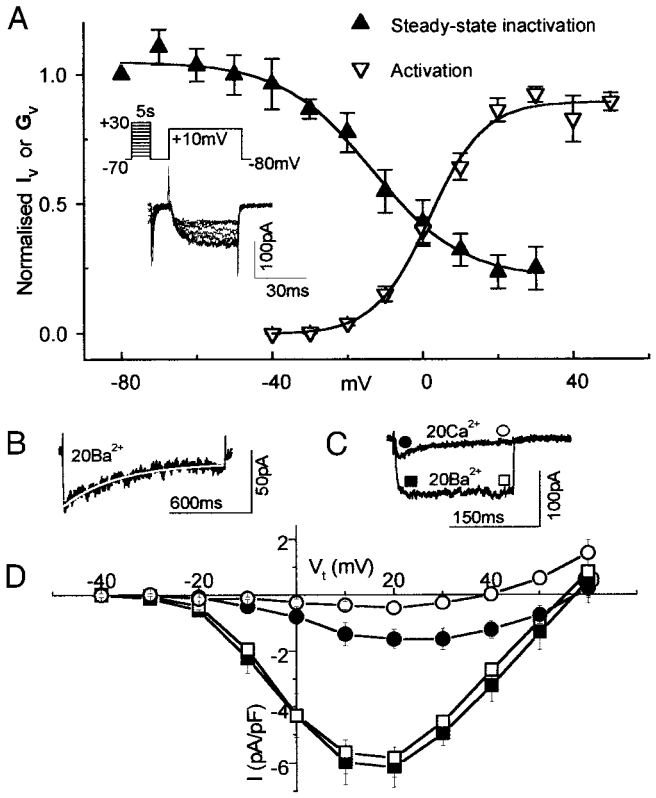

FIG. 2. Biophysical properties of α_{1D} currents. *A*: activation and steady-state inactivation curves of α_{1D} currents in 20 mM Ba^{2+}. To determine the steady-state inactivation (▲) a standard +10-mV test pulse for 40 ms was elicited from $V_h = -80$ mV, and was then preceded by a 5-s (steady-state) incremental depolarization from −70 to +30 mV every 20 s (depicted in the pulse protocol, which lies above an example family of traces for such a protocol; see *inset traces*). Peak currents were normalized to the current measured with no prepulse (mean ± SE; $n = 6$). The resulting steady-state inactivation curve was then fitted with a Boltzmann equation (*Eq. 2*, see METHODS). The fit gave the steady-state inactivation $V_{50,inact} = -13.4 \pm 1.8$ mV, and $k = 11.9 \pm 1.7$ mV. The activation (σ) was calculated using the following equation $G_V = I_V/(V - V_{rev})$. G_V and I_V are the conductance and current measured at each voltage, *V*, in the *I-V* relationship pulse protocol (see Fig. 1*D*). The *I-V* relationships were fitted with a combined Boltzmann and linear fit (*Eq. 1*, see METHODS) to determine V_{rev}. The resulting G_V values were normalized to the peak G_{max} for each *I-V* relationship, and averaged (mean ± SE; $n = 10$). The resulting data points were fitted with a Boltzmann equation (*Eq. 2*, see METHODS). The fit gave the activation $V_{50,act} = +1.8 \pm 1.2$ mV, and $k = 7.3 \pm 1.1$ mV. *B–D*: comparison of α_{1D} currents in 20 mM Ba^{2+} vs. 20 mM Ca^{2+}. *B*: long test pulses (1,200–1,600 ms) were used to determine τ_{inact} in Ba^{2+}. An example of such a fit is shown for a trace recorded in 20 mM Ba^{2+} with a +10-mV, 1,200-ms test pulse; this gave a τ_{inact} of 436 ms. *C*: example traces in Ba^{2+} and Ca^{2+} obtained by depolarizing the cells to $V_t = +10$ mV for 200 ms in each condition. By fitting a single exponential to the inactivation of the trace recorded in Ca^{2+}, a τ_{inact} of 39.1 ms was obtained. *D*: using the same *I-V* pulse protocol described in Fig. 1*D* (depolarizing from $V_h = -80$ mV to between $V_t = -40$ and +60 mV in 10-mV increments), *I-V* relationships from 6 cells were measured in 20 mM Ba^{2+} and then in 20 mM Ca^{2+}. Measurements for Ba^{2+} (peak, ■; end of pulse, □) and Ca^{2+} (peak, ●; end of pulse, ○) were made and plotted against the V_t to give the *I-V* relationship.

and associated example traces) and with 2 mM GDP-βS intracellularly (white columns and associated example traces). It can be seen in both the histogram and also in the example traces relating to these +PP/no PP ratios (Fig. 5*A*), that there was a small degree of facilitation (+PP/no PP ratio >1) in all of the intracellular conditions. Furthermore, the activation time to 90% peak (ttp 90%) was shorter for all +PP than no PP currents (Fig. 5*B*). However, the magnitude of prepulse facilitation, and the activation ttp 90%, were unaltered by inclusion of GTP-γS or GDP-βS.

In comparison, in recordings made from cells transfected with α_{1B} channels, there was no evidence of prepulse facilitation of α_{1B} currents using control intracellular pipette solution. However, following direct activation of G-proteins with GTP-γS (Fig. 5*C*), there was a marked facilitation of the +PP current compared with the no PP current. Under these recording conditions, the ttp 90% was also greater in the no PP current than in the current preceded by a prepulse, whereas in control conditions this was not apparent (Fig. 5*D*).

G-protein modulation of calcium currents can be also identified by a decrease in the current amplitude and a depolarizing shift of the *I-V* relationship with intracellular GTP-γS, while opposite effects (increase in current density and hyperpolarizing shift of the *I-V* relationship) are seen with GDP-βS (due to removal of tonic G-protein modulation). However, in the HEK

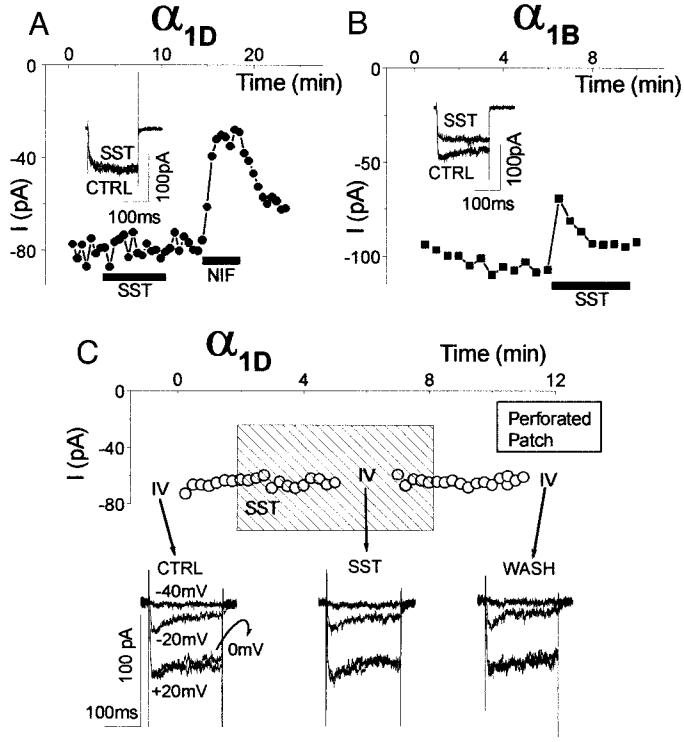

FIG. 3. The lack of G-protein–coupled receptor (endogenous sst2) modulation of α_{1D} currents. *A*: a time course of peak α_{1D} currents from whole cell patch-clamp recording. Currents were evoked every 30 s from $V_h = -80$ mV to $V_t = +10$ mV (●) in α_{1D} expressing cells in 20 mM Ba^{2+}. Somatostatin (SST; 500 nM) and NIF (3 μM) application are denoted by the horizontal bars. No response was observed in response to SST application (100–500 nM, $n = 8$). The *insets* show overlapping example traces observed in control (CTRL) and SST (500 nM). *B*: peak currents measured from whole cell patch-clamp recordings in $\alpha_{1B}/\alpha_2\delta\text{-}1/\beta_3$ expressing cells ($V_h = -80$ mV, $V_t = +20$ mV, every 30 s, ■). SST (500 nM) application inhibited the current by 40 ± 7% ($n = 8$). *Inset* shows example traces in control and during SST inhibition. *C*: peak currents measured during an amphotericin-B perforated patch-clamp experiment. Time course of peak α_{1D} currents evoked in 20 mM Ba^{2+} by depolarizing from $V_h = -80$ mV to $V_t = +10$ mV every 30 s. Application of somatostatin (SST, 500 nM) is denoted by the hatched box area. During this time course *I-V* relationships were performed in CTRL, SST, and WASH conditions (denoted by "IV" during the time course). Below the time course are examples of families of traces evoked by the standard *I-V* pulse protocol (depolarizing from $V_h = -80$ mV to between −40 and +60 mV in 10-mV increments) for CTRL, SST, and WASH conditions (for clarity examples only from $V_t = -40$, −20, 0, and +20 mV are shown).

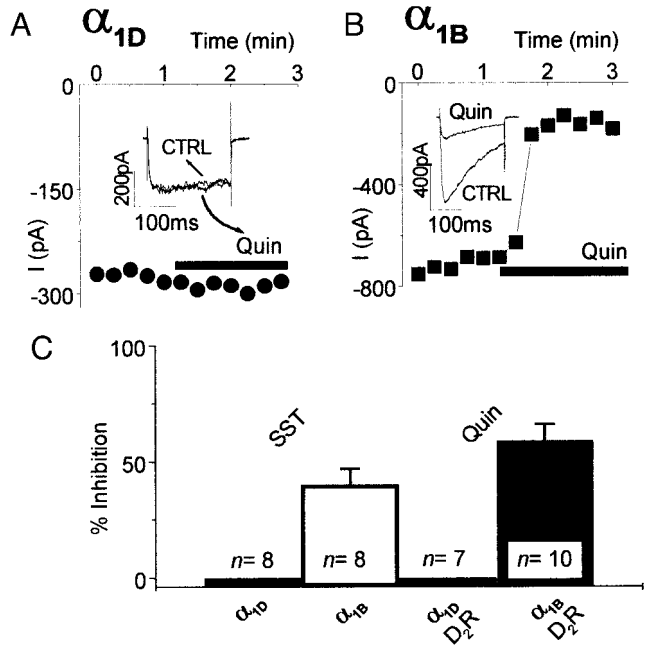

FIG. 4. The lack of G-protein–coupled receptor (transiently expressed rD_2R) modulation of α1D currents: whole cell recordings. *A*: α_{1D} expressing cells were co-transfected with $rD2_{long}$ receptor and GFP (expression marker); application of the D2 agonist quinpirole (Quin, 300 nM) had no effect on current ($n = 7$, ●); test pulses (from $V_h = -80$ mV to $V_t = +10$ mV) were given every 15 s. Traces during Quin and control (CTRL) conditions are shown in the *inset* (overlapping). *B*: transient expression of $\alpha_{1B}/\alpha_2\delta$-1/$\beta_3$ and co-expression $rD2_{long}$ receptor: time course of measured peak current (same pulse protocol as in *A*, except $V_t = +20$ mV, ■): application of Quin (300 nM) inhibited I_{Ba} in 10/16 cells tested. Example traces during CTRL and Quin application are shown in the *inset*. *C*: bar graph showing %inhibition (mean ± SE) for SST application on α_{1D} and α_{1B} currents (1st 2 columns), and for Quin on α_{1D} and α_{1B} currents (additionally co-transfected with $rD2_{long}$ receptor; 3rd and 4th columns, respectively).

293 α_{1D} cell line no difference was observed in the *I-V* relationships across the G-protein activating conditions (control, $n = 21$; +GTP-γS, $n = 23$; +GDP-βS, $n = 17$; data not shown).

α_{1D} Currents are also resistant to G-protein modulation in the presence of a 1,4-DHP agonist

In a recent study by Hernandez-Guijo et al. (1999), a form of voltage-independent G-protein modulation was observed of rat chromaffin cell L-type currents. Inhibition was observed during perfusion of a cocktail of BayK S-(−)8644, by a combination of a number of receptor agonists including ATP, opioids with or without the additional inclusion of catecholamines. In Fig. 6, we investigated whether there was any G-protein modulation of the α_{1D} currents during BayK S-(−)8644 perfusion. The α_{1D} expressing cells were also transiently transfected with rD_{2long} receptors, and after enhancement of the α_{1D} current by BayK S-(−)8644 (3 μM), a cocktail of BayK S-(−)8644 (3 μM), SST (500 nM), and quinpirole (300 nM) was applied. No effect was observed of this cocktail of drugs ($n = 5$, Figs. 6, *A* and *B*).

Selectivity of 1,4-DHP antagonists for L-type currents

Despite the lack of G-protein modulation of expressed α_{1D} channel currents in HEK 293 cells, several reports showing the modulation of 1,4-DHP–sensitive currents in neuroendocrine cells have appeared (Degtiar et al. 1997; Gilon et al. 1997; Haws et al. 1993; Hernandez-Guijo et al. 1999; Kleuss et al. 1991; Tallent et al. 1996). One possible explanation is that 1,4-DHPs may be blocking non–L-type currents, and it is these currents that exhibit the G-protein modulation. Previous re-

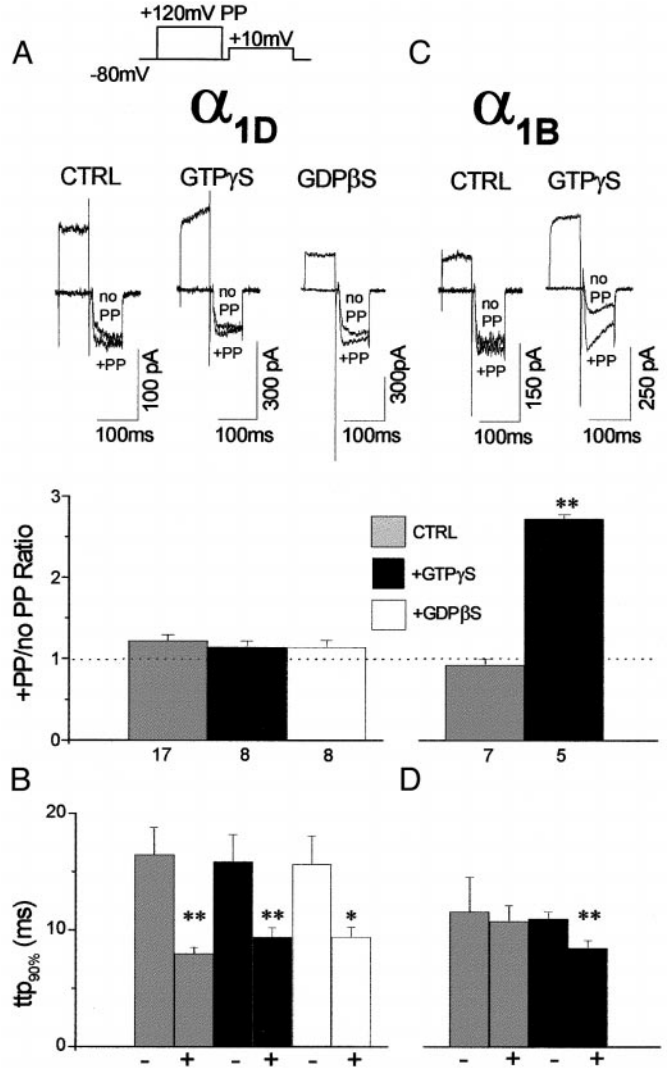

FIG. 5. Lack of G-protein modulation of α_{1D} via GTP-γS and GDP-βS. The following shading is used in all histograms: control intracellular (CTRL, gray), with 100 μM GTP-γS (+GTP-γS, black) and with 2 mM GDP-βS (+GDP-βS, white). *A* and *C*: using the pulse protocol depicted in the *top right*, in which the test pulse was applied either preceded (+PP) or not (no PP) by a 100-ms prepulse to +120 mV. The measurements of (+PP/no PP) ratio were measured in CTRL, +GTP-γS, and +GDP-βS for cells expressing α_{1D} (*A*) and α_{1B} (*C*). The +PP/no PP ratios were calculated by measuring the values of I_{Ba} at 20 ms after the start of the test pulse. Figures below columns denote the numbers of experiments. Statistical significance was determined by using an unpaired Student's *t*-test (**$P < 0.01$) between CTRL and experimental conditions. Example traces for no PP and +PP in α_{1D} with CTRL, +GTP-γS and +GDP-βS intracellular conditions are shown at the top of *A* and in α_{1B} with CTRL and +GTP-γS intracellular conditions at the top of *C*. *B* and *D*: using the same cells used for the +PP/no PP determination in *A* and *C*, the ttp 90% was measured for both sets of currents. The ttp 90% values were measured by determining the maximum current amplitude, and measuring the time at which the current reached 90% of its maximum amplitude. Statistical significance was determined using a paired Student's *t*-test between the ttp90% for no PP (−) and + PP (+) currents, for each of the conditions (*$P < 0.05$, **$P < 0.01$).

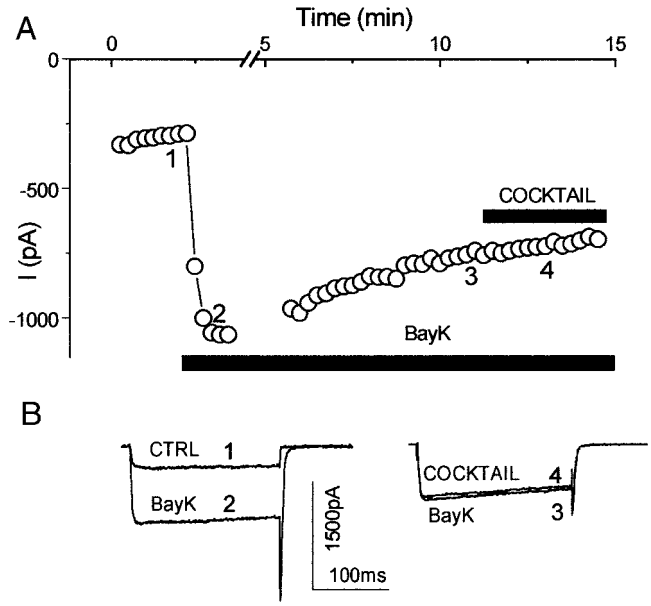

FIG. 6. α_{1D} does not exhibit sensitivity to a cocktail of SST and Quin in the presence of a DHP agonist. *A*: time course of measured peak currents in α_{1D} expressing cells ($V_h = -80$ mV, $V_t = +10$ mV every 15 s). Application of BayK S-(−)8644 (BayK, 3 μM) and the receptor agonist cocktail are depicted by the horizontal bars. The cocktail consisted of BayK (3 mM), SST (500 nM), and Quin (300 nM) and had no effect on α_{1D} currents ($n = 5$). *B*: example traces taken from the time course are denoted by numbers (*1–4*); *left*: CTRL (1) vs. current enhanced by BayK (2); *right*: overlapping currents for BayK (3) vs. cocktail (4) application.

search has shown that the selectivity of DHP antagonists for L-type channels may not be as absolute as previously thought (Diochot et al. 1995; Furukawa et al. 1999). To further examine this possibility of α_{1E} channels providing a G-protein–modulated, 1,4-DHP–sensitive current, we investigated currents resulting from transient expression of $\alpha_{1E\ long}/\alpha_2\delta\text{-}1/\beta_{1b}$. It was observed that these α_{1E} currents were inhibited by both nifedipine and nicardipine (10 μM), although the onset of inhibition is slower than for inhibition of α_{1D} currents (data not shown). The % inhibition was compared at the peak of the current and at the end of the 200-ms depolarizing test pulse. For nifedipine, there was 13 ± 4% inhibition of the peak current and 32 ± 9% inhibition at 200 ms ($n = 9$). For nicardipine, there was 63 ± 5% inhibition of the peak current and 87 ± 7% inhibition at 200 ms ($n = 3$). Thus the increased inactivation that was associated with 1,4-DHP inhibition of α_{1D} currents is also apparent for these α_{1E} currents.

Gβγ and VDCC β subunit binding to α_1 I–II loops expressed as GST fusion proteins

To examine biochemically the basis for the lack of G-protein modulation of the α_{1D} VDCC, the cytoplasmic loops between transmembrane domains I–II of the human α_{1D} and rabbit α_{1B} clones used in this study were expressed in *Escherichia coli* as GST fusion proteins and purified as described in METHODS. The purified fusion proteins are shown after separation on 12.5% SDS-PAGE gels (Fig. 7*A*). The proteins were bound via the GST moiety to the Biacore 2000 CM5 sensor chip, as described, and GST itself was used as a control. Purified bovine brain Gβγ subunits were then applied to the sensor chip surface at a rate of 50 μl/min, for 5 min. The sensorgram traces are shown in Fig. 7*B*, for three concentrations (10, 25, and 50 nM) of Gβγ exposed to the α_{1B} I–II loop, and a single concentration of Gβγ (100 nM) exposed to the α_{1D} I–II loop. In contrast to the data for the α_{1B} I–II loop, which showed concentration-dependent binding of Gβγ, no binding of Gβγ was observed to the α_{1D} I–II loop. A similar lack of binding was observed for up to 4 μM Gβγ exposed to a fusion protein of the I–II loop from a rat pancreatic α_{1D} clone (D38101, results not shown).

Kinetic analysis was performed for the lowest concentration of Gβγ (10 nM) binding to the α_{1B} I–II loop. Single exponential fits were made to the binding and dissociation phases of the sensorgram (Fig. 7*B*). The observed on-rate [$k_{on(obs)}$] for Gβγ binding was 0.0121 s^{-1}, and the off-rate (k_{off}) after termination of Gβγ perfusion was 0.0104 s^{-1}. Assuming a unimolecular reaction in which

$$k_{on(obs)} = k_{on}[G\beta\gamma] + k_{off}$$

and

$$K_D = k_{off}/k_{on}$$

the K_D for Gβγ binding was calculated to be 62.2 nM. This is very similar to the K_D determined previously for Gβγ binding to parts of the α_{1A} I–II loop (De Waard et al. 1997).

As a positive control for the integrity of the GST fusion proteins, the ability of purified H6Cβ_{1b} (Fig. 7*A*) to bind to the same I–II loops was examined. Both α_{1D} and α_{1B} I–II loops bound H6Cβ_{1b} reversibly (Fig. 7*C*), with the α_{1D} I–II loop demonstrating a higher binding affinity with a K_D of 10 nM compared with 21 nM for α_{1B}, determined as above, using the Biacore kinetic analysis software with 1:1 interaction.

DISCUSSION

L-type current characteristics exhibited by expression of the human neuronal α_{1D} clone

There are a number of key characteristics shown by the calcium channel currents expressed by the HEK 293 α_{1D} cells that are acknowledged as being traits of L-type currents. Sensitivity to the DHP antagonists (nifedipine and nicardipine) and an agonist [BayK S-(−)8644] were observed. The degree of inhibition and enhancement are comparable with other studies investigating the pharmacology of expressed cloned L-type channels (Tomlinson et al. 1993; Williams et al. 1992). In addition, the increased inactivation observed during DHP antagonist application that has been reported previously for native cardiac L-type channels (Lee and Tsien 1983) was also apparent for the α_{1D} currents. This effect of DHP antagonists on the inactivation kinetics was recently investigated by Handrock et al. (1999), who suggested that it is due to a second DHP binding site. However, care must be taken when using the characteristics of antagonism by DHPs, since, as was observed by the application of nifedipine and nicardipine to cells transiently expressing α_{1E} channels in this study, α_{1E} channels also exhibit inhibition by DHP antagonists (Stephens et al. 1997), including the characteristic increase in inactivation (compare peak inhibition with that at 200 ms into the depolarizing prepulse). More selective pharmacological definition of L-type over α_{1E} or other non–L-type currents might be obtained by using low micromolar concentrations of nifedipine (rather than

the more promiscuous nicardipine; an effect also observed in oocytes) (Furukawa et al. 1999). However, in the present study, 10 μM nifedipine was required to completely inhibit α_{1D} currents. Enhancement by BayK S-(−)8644 remains a defining characteristic of L-type currents, since α_{1E} currents have previously been shown to be insensitive to BayK S-(−)8644 (Stephens et al. 1997).

Many of the biophysical characteristics expected of L-type currents are also observed for the α_{1D} currents. The *I-V* relationship in Fig. 2*D* shows that the currents activate at about −20 mV and with the peak at approximately +20 mV in 20 mM Ba^{2+}, as also observed for other native L-type channels, and for α_{1C} currents (Lacinova et al. 1995). However, native α_{1D} currents observed in inner hair cells were shown to have *I-V* relationships approximately 20 mV negative to the *I-V* relationship observed in this study (Platzer et al. 2000); this difference may be partially accounted for by the lower external Ba^{2+} concentration used (10 mM). They also exhibit the ion selectivity ($Ba^{2+} > Ca^{2+}$) typical of other native and cloned L-type channels (Kalman et al. 1988), with current density in 20 mM Ba^{2+} being approximately five-fold greater than that seen for 20 mM Ca^{2+}. The activation observed for the α_{1D} currents expressed in this study ($V_{50,act}$ of +1.8 mV; see Fig. 2*A*) is very similar to expressed cardiac (Pérez-García et al. 1995) and neuronal (Tomlinson et al. 1993) α_{1C} L-type channel currents. The steady-state inactivation ($V_{50,inact}$ of −13.9 mV; see Fig. 2*A*), is also comparable to expressed cardiac α_{1C} L-type currents (Lacinova et al. 1995). The inactivation kinetics are also typical of "long-lasting" neuronal L-type currents (Nowycky et al. 1985). In 20 mM Ba^{2+}, very little inactivation of α_{1D} currents was observed, while rapid and striking calcium-dependent inactivation was observed in 20 mM Ca^{2+} (see Fig. 2, *B–D*).

Another characteristic of the α_{1D} currents that correlates well with other studies of expressed α_{1C} channels (Dai et al. 1999; Kamp et al. 2000) is the small but reproducible facilitation following a large depolarizing prepulse (see Fig. 5). Such attributes are often indicative of G-protein modulation; however, for the α_{1D} current this effect was independent of G-protein modulation, as it was similar in the presence of GTP-γS and GDP-βS.

As yet there are no biophysical characteristics or pharmacological tools that can differentiate between currents resulting from either native or expressed α_{1C} and α_{1D} channels. Previous research has shown that the block by DHP antagonists is voltage dependent, with greater inhibition being observed when the holding potential is more depolarized (Sanguinetti and Kass 1984). However, for the α_{1D} currents no such voltage dependence of block by DHP antagonists was observed, with similar block occurring (at both peak current and 200 ms) at all holding potentials examined. Another aspect that may prove to be different is the τ_{inact} of α_{1D} currents in Ba^{2+}. In a previous study examining the τ_{inact} of α_{1C} when co-expressed with β_3 in *Xenopus laevis* oocytes (Soldatov et al. 1997), slower rates of

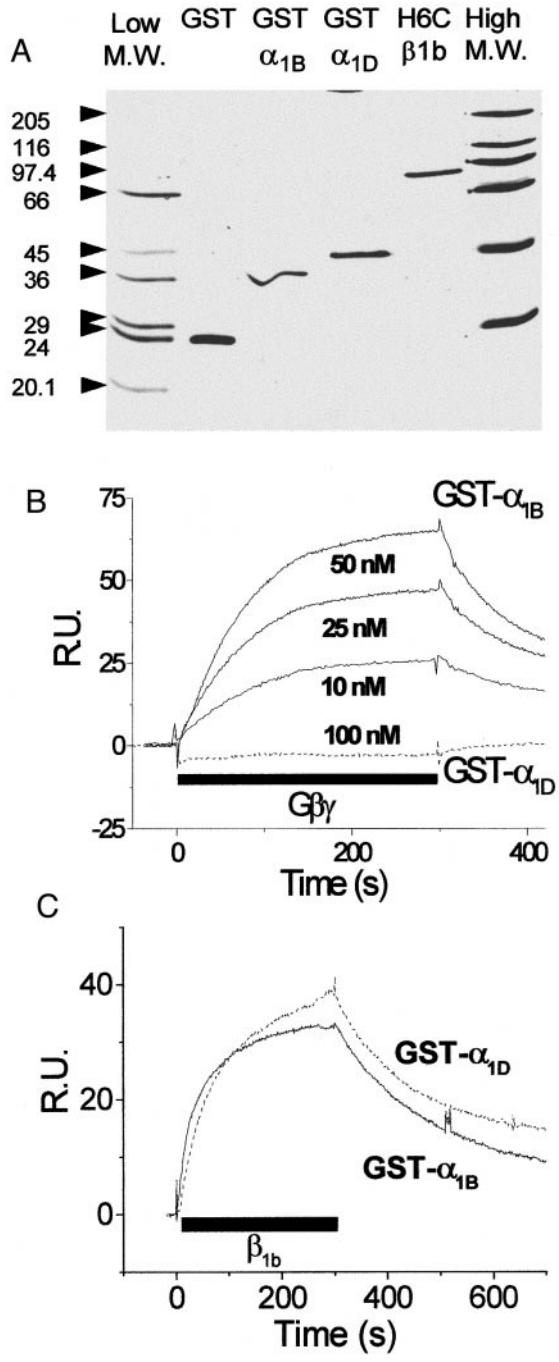

FIG. 7. Lack of G$\beta\gamma$ binding and binding of voltage-dependent calcium channel (VDCC) β subunit to α_{1D} I–II loop. *A*: silver-stained SDS gel (12.5%) (Brabet et al. 1988) of the proteins used in the surface plasmon resonance binding assays. Approximately 0.5 μg was loaded of the following proteins: GST, GSTα_{1B}I–II loop and GSTα_{1D}I–II loop, and VDCC β_{1b} subunit, as indicated. The positions of molecular mass markers (Sigma) are shown for comparison in the outside lanes. *B*: Biacore 2000 sensorgrams. Approximately 4 fmol of each fusion protein was immobilized on an individual flow cell of a CM5 dextran sensor chip via an anti-GST monoclonal antibody according to the manufacturer's instructions. This corresponds to approximately 100 reference units (R.U.) of GST, 157 R.U. of GST α_{1B}I–II loop, and 152 R.U. of GSTα_{1D}I–II loop. G$\beta\gamma$ dimers were diluted to the concentrations stated, in HBS-EP buffer before use and injected over all flow cells at a flow rate of 50 μl/min for 5 min. The resulting sensorgrams from the flow cell containing GST were subtracted from those containing the GSTα_{1B}I–II loop (solid line) and GST*h*α_{1D}I–II loop (dashed line) as a correction for bulk refractive index changes during G$\beta\gamma$ perfusion and for nonspecific binding of the G$\beta\gamma$ analyte to the GST moieties of the fusion proteins. *C*: Biacore 2000 sensorgrams for β_{1b} binding to the α_{1B} and α_{1D} I–II loop GST fusion proteins immobilized as in *B*. β_{1b} was applied at 10 nM to the α_{1D} I–II loop and 100 nM to the α_{1B} I–II loop in HBS-EP buffer containing 500 nM NaCl, at 50 μl/ml for 5 min. The data were subjected to the same subtraction procedure as described in *B*. Solid line, α_{1B} I–II loop; dashed line, α_{1D} I–II loop.

inactivation were observed (~1,300 ms) than seen here for α_{1D} currents. Nevertheless, care must be taken in interpreting such results since expression system (oocyte vs. HEK 293) and specific accessory subunit composition (particularly β subunits) will have marked effects on the inactivation properties.

Lack of G-protein modulation of α_{1D} currents

The preceding biophysical and pharmacological characterization clearly defined the α_{1D} currents as being L-type in nature. We then investigated the possibility of G-protein modulation of this L-type current. G-protein modulation was examined either by activation of the endogenous sst2 receptors or by transient expression of another GPCR, the rD_{2long} receptor. However, no modulation was observed of α_{1D} currents via either pathway. To ensure that the G-protein pathways were intact and capable of coupling to calcium channels in the HEK 293 cells, both the endogenous sst2 and the transiently expressed exogenous $rD2_{long}$ receptors were stimulated via their respective agonists in HEK 293 cells expressing α_{1B} currents, which have been shown to be G-protein modulated by many groups (for review, see Dolphin 1998). These positive controls showed obvious G-protein modulation, confirming that modulation is possible by these pathways. Furthermore, the modulation of the α_{1D} current was also investigated during application of BayK S-(−)8644, since G-protein–mediated inhibition of L-type currents had been observed in native rat chromaffin cells, during enhancement by BayK S-(−)8644 (Hernandez-Guijo et al. 1999). However, a combination of BayK S-(−)8644, SST, and quinpirole did not reveal inhibitory G-protein modulation of BayK S-(−)8644–enhanced α_{1D} currents co-expressed with $rD2_{long}$ (see Fig. 6).

Another method to examine G-protein modulation is to use the nonhydrolyzable GTP and GDP analogues GTP-γS and GDP-βS. The advantage of using these guanine nucleotide analogues is that they act directly on all G-proteins, producing sustained activation (in the case of GTP-γS) or blockade of activation (GDP-βS) (Dolphin and Scott 1987). Using a standard large depolarizing (+120 mV) prepulse protocol to detect G-protein modulation, no GTP-γS–dependent effect was observed on α_{1D} currents, yet the α_{1B} currents do exhibit marked tonic G-protein modulation in these conditions.

The lack of G-protein modulation of this α_{1D} clone is corroborated by the lack of G$\beta\gamma$ binding to a GST fusion protein of the α_{1D} I–II loop, whereas in parallel experiments, reversible binding of G$\beta\gamma$ was observed to the α_{1B} I–II loop. In contrast, both the α_{1D} and α_{1B} I–II loops reversibly bound purified β_{1b} subunit, indicating that they are probably folded in a native conformation (see Fig. 7*C*). While the I–II loop is not the only region of the α_{1B} calcium channel that is involved in its G-protein regulation (Canti et al. 1999; Page et al. 1998; Zhang et al. 1996), nevertheless it is certainly one of the key sequences contributing to the inhibition of neuronal calcium channels (De Waard et al. 1997).

G_s-protein modulation of L-type currents was also investigated by activation of the G_s-adenyl cyclase pathway with forskolin. No effect of forskolin was observed ($n = 4$, data not shown). Protein kinase A (PKA) modulation of channels has been shown to require A-kinase anchoring proteins (AKAPs) (Johnson et al. 1997). The presence of AKAPs was not examined in this study, although they are likely to be present since they are found in tsA-201 cells which are an HEK 293–derived cell line (Johnson et al. 1997).

From these results, the α_{1D} L-type clone used in the present study does not appear to be the molecular counterpart of the native neuronal and endocrine L-type channels that have been shown to exhibit G-protein modulation in several neuroendocrine preparations (Degtiar et al. 1997; Gilon et al. 1997; Haws et al. 1993; Hernandez-Guijo et al. 1999; Kleuss et al. 1991; Tallent et al. 1996).

Source of G-protein–modulated neuroendocrine L-type current?

Since we have shown that the $\alpha_{1D}/\alpha_2\delta\text{-}1/\beta_{3a}$ currents do not exhibit inhibitory G-protein modulation, what is the molecular counterpart of the native L-type current in neuroendocrine cells that do exhibit G-protein modulation? L-type currents are generally identified by their sensitivity to DHP antagonists; however, we previously demonstrated DHP antagonist block of a rat α_{1E} isoform, rbEII (Stephens et al. 1997). Because this isoform has a 50 amino acid truncation of the N-terminus compared with α_{1E} clones from other species (Page et al. 1998), and may therefore not represent a native isoform in rat brain (Schramm et al. 1999), we have now confirmed and extended the finding of DHP sensitivity of α_{1E} currents, using α_{1Elong}, an isoform whose extended N-terminus is homologous to the cloned human (L27745), rabbit (X67855), and mouse (L29346) (Williams et al. 1994) α_{1E} sequences. The partial DHP sensitivity (particularly to nicardipine) of α_{1E} currents observed, as well as the DHP sensitivity of other cloned non–L-type currents observed recently (Furukawa et al. 1999) suggests the caveat that some studies apparently demonstrating G-protein modulation of "L-type" currents (according to their sensitivity to DHP antagonists) may need to be reviewed. However, this uncertainty over identification of L-type currents by DHP antagonist sensitivity may only be relevant to a few studies, and the significant bank of evidence for G-protein modulation of neuroendocrine L-type channels will be unaffected, particularly those studies in which L-type currents have been defined by S(−)-BayK8644 enhancement (Hernandez-Guijo et al. 1999).

Additional α_{1D} isoforms have been cloned from pancreatic β-cells in rat (Ihara et al. 1995) and hamster (Yaney et al. 1992). There is little functional expression data available for these clones. Expression of α_{1D} clones appears to be problematic with relatively low current density yields (even in the clone used in this study, a low percentage of cells exhibited stable currents), a problem that has hindered research in this area and may indicate that the full-length clones currently available are not naturally occurring splice variants. A number of sequences within the α_{1A}, α_{1B}, and α_{1E} VDCC subunits have been shown to be important for $G_{\beta\gamma}$ binding and modulation of the channel. These important α_1 VDCC subunit sequences include the intracellular loop between domains I and II (De Waard et al. 1997), a region within the N-terminus (Canti et al. 1999; Page et al. 1998) and the C-terminus (Qin et al. 1997; Zhang et al. 1996). Two particularly relevant motifs present in the I–II loop (QQIER) (Zamponi et al. 1997) and the N-terminus (YKQSIAQRART) (Canti et al. 1999) of α_{1B} are not conserved in the α_{1D} clone used here. Furthermore, when comparing sequence alignments of the pancreatic β-cell α_{1D} clones with the neu-

ronal α_{1D} clone used in this study, most elements in putative regions pertinent to G-protein modulation are homologous to each other. This suggests that these additional published α_{1D} clones may also be predicted to exhibit no G-protein modulation. Indeed, similar results have been obtained regarding the lack of inhibitory G-protein modulation of another α_{1D} clone (Yaney et al. 1992) (A. Scholze, T. D. Plant, A. C. Dolphin, and B. Nürnberg, unpublished results). However, the α_{1D} sequences show least conservation in the C-terminal tails, with either long (as in the α_{1D} clone used here) or short C-terminus isoforms (as in Yaney et al. 1992) providing scope for the possibility that the C-terminus of alternative α_{1D} splice variants may provide a means of G-protein modulation of certain splice variants.

As further progress is made in the elucidation of neuroendocrine L-type channels, it is becoming clear that a sophisticated level of complexity is likely to exist. For example, in the GH_3 (a rat pituitary derived) cell line alone, several mRNA transcripts encoding splice variants of the α_{1D} subunit have been reported (Safa et al. 1998). Further complexity of these channels will be added due to the differing combinations of accessory subunits. Although β_3 appears to be a significant accessory subunit associated with neuronal L-type channels (Pichler et al. 1997), nevertheless, β_4 is also prominently associated with neuronal L-type channels, and β_{1b} and β_{2a} are also associated with a small proportion of the channels (Pichler et al. 1997). Between β subunit isoforms there are also splice variants (for reviews see Birnbaumer et al. 1998; Castellano and Perez-Reyes 1994) that add to the channel subunit complexity. Among these combinations of α_{1D} splice variants and accessory subunits, there may be a sub-set that do exhibit the G-protein modulation observed in native neuroendocrine cells and derived cell lines. Alternatively, an as yet undiscovered accessory protein may be required for coupling of the neuronal L-type channels to G-protein inhibitory pathways, or modulation may involve Ca^{2+}-dependent mechanisms (Mathie et al. 1992), a process not investigated in the present study.

The cDNAs used in this study were generously provided by the following: E. Perez-Reyes (University of Virginia); T. Snutch (University of British Columbia, Vancouver, Canada); Y. Mori (Seriken, Okazaki, Japan); P. G. Strange (Reading, UK); T. Hughes (Yale, New Haven, CT); and Genetics Institute (Cambridge, MA). The technical help of N. Balaguero is gratefully acknowledged.

This work was supported by the Medical Research Council (MRC), Wellcome Trust and Royal Society. D. C. Bell was funded by a MRC/Merck, Sharp and Dohme collaborative Ph.D. studentship.

Present addresses: D. C. Bell, Center for Neurobiology and Behavior, Columbia University, New York, NY 10032; P. F. Brust, Ambryx Inc., 11099 N. Torrey Pines Rd., #160, La Jolla, CA 92037; A. Nesterova, Dept. of Endocrinology, University of Colorado Health Sciences Center, Denver, CO 80262.

REFERENCES

BEAN BP. Neurotransmitter inhibition of neuronal calcium currents by changes in channel voltage-dependence. *Nature* 340: 153–155, 1989.

BIRNBAUMER L, QIN N, OLCESE R, TAREILUS E, PLATANO D, COSTANTIN J, AND STEFANI E. Structures and functions of calcium channel β subunits. *J Bioenerg Biomembr* 30: 357–375, 1998.

BOURINET E, SOONG TW, STEA A, AND SNUTCH TP. Determinants of the G-protein–dependent opioid modulation of neuronal calcium channels. *Proc Natl Acad Sci USA* 93: 1486–1491, 1996.

BRABET E, PANTALONI C, ROUOT B, TOUTANT M, GARCIA-SAINZ A, BOCKAERT J, AND HOMBURGER V. Multiple species and isoforms of *Bordatella* pertussis toxin substrates. *Biochem Biophys Res Commun* 152: 1185–1192, 1988.

BRUST PF, SIMERSON S, MCCUE AF, DEAL CR, SCHOONMAKER S, WILLIAMS ME, VELIÇELEBI G, JOHNSON EC, HARPOLD MM, AND ELLIS SB. Human neuronal voltage-dependent calcium channels: studies on subunit structure and role in channel assembly. *Neuropharmacology* 32: 1089–1102, 1993.

CAMPBELL V, BERROW NS, FITZGERALD EM, BRICKLEY K, AND DOLPHIN AC. Inhibition of the interaction of G-protein G_o with calcium channels by the calcium channel β-subunit in rat neurones. *J Physiol (Lond)* 485: 365–372, 1995.

CANTI C, PAGE KM, STEPHENS GJ, AND DOLPHIN AC. Identification of residues in the N terminus of α_{1B} critical for inhibition of the voltage-dependent calcium channel by G$\beta\gamma$. *J Neurosci* 19: 6855–6864, 1999.

CASTELLANO A AND PEREZ-REYES E. Molecular diversity of Ca^{2+} channel β subunits. *Biochem Soc Trans* 22: 483–488, 1994.

CHIN H, SMITH MA, KIM H-L, AND KIM H. Expression of dihydropyridine-sensitive brain calcium channels in the rat central nervous system. *FEBS Lett* 299: 69–74, 1992.

DAI S, KLUGBAUER N, ZONG X, SEISENBERGER C, AND HOFMANN F. The role of subunit composition on prepulse facilitation of the cardiac L-type calcium channel. *FEBS Lett* 442: 70–74, 1999.

DEGTIAR VE, HARHAMMER R, AND NÜRNBERG B. Receptors couple to L-type calcium channels via distinct G_o proteins in rat neuroendocrine cell lines. *J Physiol (Lond)* 502: 321–333, 1997.

DE WAARD M, LIU HY, WALKER D, SCOTT VES, GURNETT CA, AND CAMPBELL KP. Direct binding of G-protein $\beta\gamma$ complex to voltage-dependent calcium channels. *Nature* 385: 446–450, 1997.

DIOCHOT S, RICHARD S, BALDY-MOULINIER M, NARGEOT J, AND VALMIER J. Dihydropyridines, phenylalkylamines and benzothiazepines block N-, P/Q- and R-type calcium currents. *Pflügers Arch* 431: 10–19, 1995.

DOLPHIN AC. Mechanisms of modulation of voltage-dependent calcium channels by G-proteins. *J Physiol (Lond)* 506: 3–11, 1998.

DOLPHIN AC. L-type calcium channel modulation. In: *Advances in Second Messenger and Phosphoprotein Research, 33*, edited by Armstrong DL and Rossie S. San Diego, CA: Academic, 1999, p. 153–177.

DOLPHIN AC AND SCOTT RH. Calcium channel currents and their inhibition by (−)-baclofen in rat sensory neurones: modulation by guanine nucleotides. *J Physiol (Lond)* 386: 1–17, 1987.

ELMSLIE KS, ZHOU W, AND JONES SW. LHRH and GTPγ S modify calcium current activation in bullfrog sympathetic neurons. *Neuron* 5: 75–80, 1990.

ERTEL EA, CAMPBELL KP, HARPOLD MM, HOFMANN F, MORI Y, PEREZ-REYES E, SCHWARTZ A, SNUTCH TP, TANABE T, BIRNBAUMER L, TSIEN RW, AND CATTERALL WA. Nomenclature of voltage-gated calcium channels [Letter]. *Neuron* 25: 533–535, 2000.

EXNER T, JENSEN ON, MANN M, KLEUSS C, AND NÜRNBERG B. Posttrsanslational modification of Gα_{o1} generates Gα_{o3}, an abundant G-protein in brain. *Proc Natl Acad Sci USA* 96: 1327–1332, 1999.

FISCHMEISTER R AND HARTZELL HC. Mechanism of action of acetylcholine on calcium current in single cells from frog ventricle. *J Physiol (Lond)* 376: 183–202, 1986.

FURUKAWA T, YAMAKAWA T, MIDERA T, SAGAWA T, MORI Y, AND NUKADA T. Selectivities of dihydropyridine derivatives in blocking Ca^{2+} channel subtypes expressed in *Xenopus* oocytes. *J Pharmacol Exp Ther* 291: 464–473, 1999.

GILON P, YAKEL J, GROMADA J, ZHU Y, HENQUIN JC, AND RORSMAN P. G-protein–dependent inhibition of L-type Ca^{2+} currents by acetylcholine in mouse pancreatic B-cells. *J Physiol (Lond)* 499: 65–76, 1997.

HANDROCK R, RAO-SCHYMANSKI R, KLUGBAUER N, HOFMANN F, AND HERZIG S. Dihydropyridine enantiomers block recombinant L-type Ca^{2+} channels by two different mechanisms. *J Physiol (Lond)* 521: 31–42, 1999.

HAWS CM, SLESINGER PA, AND LANSMAN JB. Dihydropyridine- and omega-conotoxin–sensitive Ca^{2+} currents in cerebellar neurons: persistent block of L-type channels by a pertussis toxin-sensitive G-protein. *J Neurosci* 13: 1148–1156, 1993.

HELL JW, WESTENBROEK RE, WARNER C, AHLIJANIAN MK, PRYSTAY W, GILBERT MM, SNUTCH TP, AND CATTERALL WA. Identification and differential subcellular localization of the neuronal class C and class D L-type calcium channel α1 subunits. *J Cell Biol* 123: 949–962, 1993.

HERLITZE S, GARCIA DE, MACKIE K, HILLE B, SCHEUER T, AND CATTERALL WA. Modulation of Ca^{2+} channels by G-protein beta gamma subunits. *Nature* 380: 258–262, 1996.

HERNANDEZ-GUIJO JM, CARABELLI V, GANDIA L, GARCIA AG, AND CARBONE E. Voltage-independent autocrine modulation of L-type channels mediated by ATP, opioids and catecholamines in rat chromaffin cells. *Eur J Neurosci* 11: 3574–3584, 1999.

HORN R AND MARTY A. Muscarinic activation of ionic currents measured by a new whole-cell recording method. *J Gen Physiol* 92: 145–159, 1988.

IHARA Y, YAMADA Y, FUJII Y, GONOI T, YANO H, YASUDA K, INAGAKI N, SEINO Y, AND SEINO S. Molecular diversity and functional characterization of voltage-dependent calcium channels (CACN4) expressed in pancreatic beta-cells. *Mol Endocrinol* 9: 121–130, 1995.

IKEDA SR. Voltage-dependent modulation of N-type calcium channels by G-protein beta gamma subunits. *Nature* 380: 255–258, 1996.

JOHNSON BD, BROUSAL JP, PETERSON BZ, GALLOMBARDO PA, HOCKERMAN GH, LAI Y, SCHEUER T, AND CATTERALL WA. Modulation of the cloned skeletal muscle L-type Ca^{2+} channel by anchored cAMP-dependent protein kinase. *J Neurosci* 17: 1243–1255, 1997.

KALMAN D, LAGUE PH, ERXLEBEN C, AND ARMSTRONG DL. Calcium-dependent inactivation of the dihydropyridine-dependent calcium channels in GH_3 cells. *J Gen Physiol* 92: 531–548, 1988.

KAMP TJ, HU H, AND MARBAN E. Voltage-dependent facilitation of cardiac L-type Ca channels expressed in HEK-293 cells requires beta-subunit. *Am J Physiol Heart Circ Physiol* 278: H126–H136, 2000.

KLEUSS C, HESCHELER J, EWEL C, ROSENTHAL W, SCHULTZ G, AND WITTIG B. Assignment of G-protein subtypes to specific receptors inducing inhibition of calcium currents. *Nature* 353: 43–48, 1991.

LACINOVA L, LUDWIG A, BOSSE E, FLOCKERZI V, AND HOFMAN F. The block of the expressed L-type calcium channel is modulated by the β_3 subunit. *FEBS Lett* 373: 103–107, 1995.

LEE KS AND TSIEN RW. Mechanism of calcium channel blockade by verapamil, D600, diltiazem and nitrendipine in single dialysed heart cells. *Nature* 302: 790–794, 1983.

MATHIE A, BERNHEIM L, AND HILLE B. Inhibition of N- and L-type calcium channels by muscarinic receptor activation in rat sympathetic neurons. *Neuron* 8: 907–914, 1992.

MEZA U AND ADAMS B. G-protein–dependent facilitation of neuronal alpha(1A), alpha(1B) and alpha(1E) Ca channels. *J Neurosci* 18: 5240–5252, 1998.

MIKAMI A, IMOTO K, TANABE T, NIIDOME T, MORI Y, TAKESHIMA H, NARUMIYA S, AND NUMA S. Primary structure and functional expression of the cardiac dihydropyridine-sensitive calcium channel. *Nature* 340: 230–233, 1989.

NEHER E. Voltage offsets in patch-clamp experiments. In: *Single-Channel Recording,* edited by Sakmann B and Neher E. New York: Plenum, 1995, p. 147–153.

NOWYCKY MC, FOX AP, AND TSIEN RW. Three types of neuronal calcium channel with different calcium agonist sensitivity. *Nature* 316: 440–446, 1985.

OZ M, MELIA MT, SOLDATOV NM, ABERNETHY DR, AND MORAD M. Functional coupling of human L-type Ca^{2+} channels and angiotensin AT(1A) receptors coexpressed in *Xenopus laevis* oocytes: involvement of the carboxyl-terminal Ca^{2+} sensors. *Mol Pharmacol* 54: 1106–1112, 1998.

PAGE KM, CANTI C, STEPHENS GJ, BERROW NS, AND DOLPHIN AC. Identification of the amino terminus of neuronal Ca^{2+} channel α_1 subunits α_{1B} and α_{1E} as an essential determinant of G-protein modulation. *J Neurosci* 18: 4815–4824, 1998.

PÉREZ-GARCÍA MT, KAMP TJ, AND MARBÁN E. Functional properties of cardiac L-type calcium channels transiently expressed in HEK293 cells. Role of α_1 and β subunits. *J Gen Physiol* 105: 289–306, 1995.

PICHLER M, CASSIDY TN, REIMER D, HAASE H, KRAUS R, OSTLER D, AND STRIESSNIG J. Beta subunit heterogeneity in neuronal L-type Ca^{2+} channels. *J Biol Chem* 272: 13877–13882, 1997.

PLATZER J, ENGEL J, SCHROTT-FISCHER A, STEPHAN K, BOVA S, CHEN H, ZHENG H, AND STRIESSNIG J. Congenital deafness and sinoatrial node dysfunction in mice lacking class D L-type Ca^{2+} channels. *Cell* 102: 89–97, 2000.

QIN N, PLATANO D, OLCESE R, STEFANI E, AND BIRNBAUMER L. Direct interaction of $G\beta\gamma$ with a C-terminal $G\beta\gamma$ binding domain of the Ca^{2+} channel α_1 subunit is responsible for channel inhibition by G-protein–coupled receptors. *Proc Natl Acad Sci USA* 94: 8866–8871, 1997.

REUTER H. Calcium channel modulation by neurotransmitters, enzymes and drugs. *Nature* 301: 569–574, 1983.

SAFA P, HALES TG, SONG L, AND BOULTER J. Multiple splice variants of alpha 1D Ca^{2+} in GH3 cells. *Soc Neurosci Abstr* 24: 83, 1998.

SANGUINETTI MC AND KASS RS. Voltage-dependent modulation of Ca channel current in the calf cardiac purkinje fiber by dihydropyridine calcium channel antagonists. *Circ Res* 55: 336–348, 1984.

SCHRAMM M, VAJNA R, PEREVERZEV A, TOTTENE A, KLÖCKNER U, PIETROBON D, HESCHELER J, AND SCHNEIDER T. Isoforms of α1E voltage-gated calcium channels in rat cerebellar granule cells—detection of major calcium channel α1-transcripts by reverse transcription-polymerase chain reaction. *Neuroscience* 92: 565–575, 1999.

SEINO S, CHEN L, SEINO M, BLONDEL O, TAKEDA J, JOHNSON JH, AND BELL GI. Cloning of the α_1 subunit of a voltage-dependent calcium channel expressed in pancreatic β cells. *Proc Natl Acad Sci USA* 89: 584–588, 1992.

SOLDATOV NM, ZÜHLKE RD, BOURON A, AND REUTER H. Molecular structures involved in L-type calcium channel inactivation—role of the carboxyl-terminal region encoded by exons 40–42 in α_{1C} subunit in the kinetics and Ca^{2+} dependence of inactivation. *J Biol Chem* 272: 3560–3566, 1997.

STEPHENS GJ, CANTI C, PAGE KM, AND DOLPHIN AC. Role of domain I of neuronal Ca^{2+} channel α 1 subunits in G-protein modulation. *J Physiol (Lond)* 509: 163–169, 1998.

STEPHENS GJ, PAGE KM, BURLEY JR, BERROW NS, AND DOLPHIN AC. Functional expression of rat brain cloned α_{1E} calcium channels in COS-7 cells. *Pflügers Arch* 433: 523–532, 1997.

STROM TM, NYAKATURA G, APFELSTEDT SYLLA E, HELLEBRAND H, LORENZ B, WEBER BH, WUTZ K, GUTWILLINGER N, RUTHER K, DRESCHER B, SAUER C, ZRENNER E, MEITINGER T, ROSENTHAL A, AND MEINDL A. An L-type calcium-channel gene mutated in incomplete X-linked congenital stationary night blindness. *Nature Genet* 19: 260–263, 1998.

SWICK AG, JANICOT M, CHENEVAL-KASTELIC T, MCLENITHAN JC, AND LANE DM. Promoter-cDNA–directed heterologous protein expression in *Xenopus laevis* oocytes. *Proc Natl Acad Sci USA* 89: 1812–1816, 1992.

TALLENT M, LIAPAKIS G, O'CARROLL AM, LOLAIT SJ, DICHTER M, AND REISINE T. Somatostatin receptor subtypes SSTR2 and SSTR5 couple negatively to an L-type Ca^{2+} current in the pituitary cell line AtT-20. *Neuroscience* 71: 1073–1081, 1996.

TANABE T, TAKESHIMA H, MIKAMI A, FLOCKERZI V, TAKAHASHI H, KANGAWA K, KOJIMA M, MATSUO H, HIROSE T, AND NUMA S. Primary structure of the receptor for calcium channel blockers from skeletal muscle. *Nature* 328: 313–318, 1987.

TOMLINSON WJ, STEA A, BOURINET E, CHARNET P, NARGEOT J, AND SNUTCH TP. Functional properties of a neuronal class C L-type calcium channel. *Neuropharmacology* 32: 1117–1126, 1993.

VIARD P, EXNER T, MAIER U, MIRONNEAU J, NURNBERG B, AND MACREZ N. $G\beta\gamma$ dimers stimulate vascular L-type Ca^{2+} channels via phosphoinositide 3-kinase. *FASEB J* 13: 685–694, 1999.

WILLIAMS ME, FELDMAN DH, MCCUE AF, BRENNER R, VELICELEBI G, ELLIS SB, AND HARPOLD MM. Structure and functional expression of α_1, α_2, and β subunits of a novel human neuronal calcium channel subtype. *Neuron* 8: 71–84, 1992.

WILLIAMS ME, MARUBIO LM, DEAL CR, HANS M, BRUST PF, PHILIPSON LH, MILLER RJ, JOHNSON EC, HARPOLD MM, AND ELLIS SB. Structure and functional characterization of neuronal α_{1E} calcium channel subtypes. *J Biol Chem* 269: 22347–22357, 1994.

WYATT CN, CAMPBELL V, BRODBECK J, BRICE NL, PAGE KM, BERROW NS, BRICKLEY K, TERRACCIANO CM, NAQVI RU, MACLEOD KT, AND DOLPHIN AC. Voltage-dependent binding and calcium channel current inhibition by an anti-alpha 1D subunit antibody in rat dorsal root ganglion neurones and guinea-pig myocytes. *J Physiol (Lond)* 502: 307–319, 1997.

YANEY GC, WHEELER MB, WEI X, PEREZ-REYES E, BIRNBAUMER L, BOYD AE III, AND MOSS LG. Cloning of a novel α_1-subunit of the voltage-dependent calcium channel from the β-cell. *Mol Endocrinol* 6: 2143–2152, 1992.

ZAMPONI JF, BOURINET E, NELSON D, NARGEOT J, AND SNUTCH TP. Crosstalk between G-proteins and protein kinase C mediated by the calcium channel α_1 subunit. *Nature* 385: 442–446, 1997.

ZHANG JF, ELLINOR PT, ALDRICH RW, AND TSIEN RW. Multiple structural elements in voltage-dependent Ca^{2+} channels support their inhibition by G-proteins. *Neuron* 17: 991–1003, 1996.